

## Review on swirl-type microbubble generator: Concept, technology, and applications

Drajat Indah Mawarni<sup>1\*</sup>, Hartono Guntur Ristiyanto<sup>2</sup>, Deendarlianto<sup>3</sup>,  
Wiratni Budhijanto<sup>4</sup>, Mai Salem<sup>5</sup>, Hakeem Niyas<sup>6</sup>, Indarto<sup>3</sup>

<sup>1</sup> Department of Mechanical Engineering, Ronggolawe Technology College of Cepu, Cepu 58315, **Indonesia**

<sup>2</sup> Department of Civil Engineering, Ronggolawe Technology College of Cepu, Cepu 58315, **Indonesia**

<sup>3</sup> Department of Mechanical and Industrial Engineering, Universitas Gadjah Mada, Yogyakarta 55281, **Indonesia**

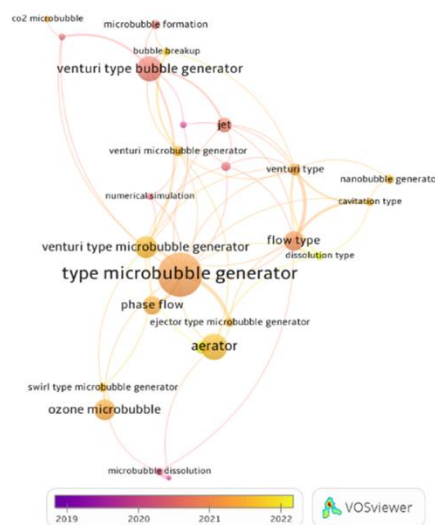
<sup>4</sup> Department of Chemical Engineering, Universitas Gadjah Mada, Yogyakarta 55281, **Indonesia**

<sup>5</sup> Egypt-Japan University of Science and Technology, Alexandria Governorate 21934, **Egypt**

<sup>6</sup> Energy Institute Bangalore, Karnataka 562157, **India**

✉ [drajatindah74@gmail.com](mailto:drajatindah74@gmail.com)

This article  
contributes to:



### Highlights:

- Microbubble Generator (MBG) is a technology for generating micron-sized bubbles that has been developed in various forms and applications.
- The swirl-type MBG has proven to be more effective in producing micron-sized bubbles and has a simpler manufacturing process.
- The influence of variables on the fluid properties or dimensions of the microbubble generator on the performance of the microbubble generator was formulated.
- Most research on microbubble generators has been conducted using clean water while the use of wastewater is still relatively limited.

### Abstract

The Microbubble Generator (MBG) is an aeration technology capable of producing micron-sized bubbles. Several researchers have conducted previous studies and developed various types related to the microbubble generator. The swirl-type microbubble generator has demonstrated advantages over other types. It has been widely explored recently due to its simple structure, efficiency in producing micron-sized bubbles, and potential applications across various fields. Therefore, this article reviews recent developments in swirl-type bubble generator research, encompassing the definition of microbubbles, methods for generating microbubbles through experimental and numerical approaches, the performance of microbubble generators, and their applications. Based on optimized geometric parameters combined with appropriate flow conditions, the swirl-type bubble generator is predicted to produce bubbles with controlled sizes and concentrations that meet specific requirements. However, further studies are needed to delineate the fluid-gas interactions comprehensively.

**Keywords:** Microbubble, Microbubble generator, Swirl-type generator

### Article info

Submitted:  
2023-11-18

Revised:  
2023-12-27

Accepted:  
2023-12-28



This work is licensed under  
a Creative Commons  
Attribution-NonCommercial 4.0  
International License

### Publisher

Universitas Muhammadiyah  
Magelang

## 1. Introduction

Microbubbles are micron-sized bubbles with a diameter smaller than one millimeter and larger than one micrometer [1]. They exhibit unique characteristics, including high gas dissolution, low rising velocity, and a high interfacial area. Researchers hold varying opinions on the definition of microbubbles. According to Tabei et al. [2], microbubbles are bubbles with a diameter of less than 100  $\mu\text{m}$  that can be evenly distributed. Sadatomi et al. [3] microbubbles as small bubbles with a diameter of less than 100  $\mu\text{m}$ , possessing high solubility in water. On the other hand, Liu an Bai

[4] defines microbubbles as bubbles with a diameter of 50-200  $\mu\text{m}$ , while Temesgen et al. [5] characterizes them as small bubbles with a size ranging from 1 to 100  $\mu\text{m}$ . Then, Juwana et al. [6] states that microbubbles have a diameter of 200  $\mu\text{m}$ , and Agarwal [7] defines microbubbles as bubbles with a diameter of 150  $\mu\text{m}$ .

Bubble flow, characterized by the intermingling of gas and liquid phases with gas or vapor present within the liquid, represents a common and fundamental pattern. This flow pattern holds significant importance across various applications due to its favorable features, including a large contact surface facilitating efficient heat and mass transfer, as well as effective mixing processes. Applications span from reducing organic pollutants, water disinfection, and cleaning solid surfaces to detoxifying water [7]. Bubble flow is also effective in eliminating diverse pollutants like colloids, fine particles, ultrafine particles, sediments, ions, microorganisms, dispersed proteins, and emulsified oils in water [8], [9]. Its versatility extends to simultaneous cleaning and preventing pollution by the same substances water purification processes utilizing bubbles with a diameter of 70 - 100  $\mu\text{m}$  [10], and enhancing mass transfer to improve water purification effectiveness [11] as reviewed by Temesgen et al. [5]. It is employed in wastewater purification [11], greywater purification processes [12], wastewater purification [12]–[15], coagulation processes in textile dye wastewater [16], purification of Palm Oil Mill Effluent (POME) [17], acting as a tracer in Particle Image Velocimetry (PIV) [18], reducing pressure waves in Helium gas [19], [20], shellfish and oyster cultivation, reducing radicals (such as antibacterial, deodorizing, liquid purification), increasing human blood flow rate during bathing with microbubble-containing water, and fermentation [21]. In the realm of biotechnology, bubble flow aids in enhancing mass transfer for improved microalgae growth rates, releases  $\text{O}_2$  through algae photosynthesis, and prevents algae from adhering to reactor walls [9].

With the increasing applications of bubble flows, controlling the size and concentration of bubbles has become a crucial issue, drawing significant attention [22], [23]. To meet diverse application requirements, various methods for producing fine bubbles have been developed. The swirl-type microbubble generator is particularly effective in generating small-sized bubbles compared to other types [2], [13], [24]. The swirl-type Microbubble Generator (MBG) consists of three main components: tangential water inlet, swirling chamber, and mixing channel. The tangential flow method has garnered significant attention for its capability to produce relatively small-sized bubbles and its simple construction, making it easily manufacturable [25]. The operational principle involves pressurized fluid being tangentially introduced into a cylinder to create a swirling flow [2], [26]. As the velocity increases, following Bernoulli's principle of energy conservation, the rise in velocity (kinetic energy) at a certain point in the flow results in reduced pressure [27]. This negative pressure formation causes air to flow through the gas nozzle due to self-suction [28]–[30]. The dimensional parameters of this type of MBG generally include the gas inlet radius, air inlet radius, outlet nozzle radius (mixing channel), and the volume of the swirl chamber. The schematic diagram of this type of MBG, as presented in the work [29], can be observed in Figure 1.

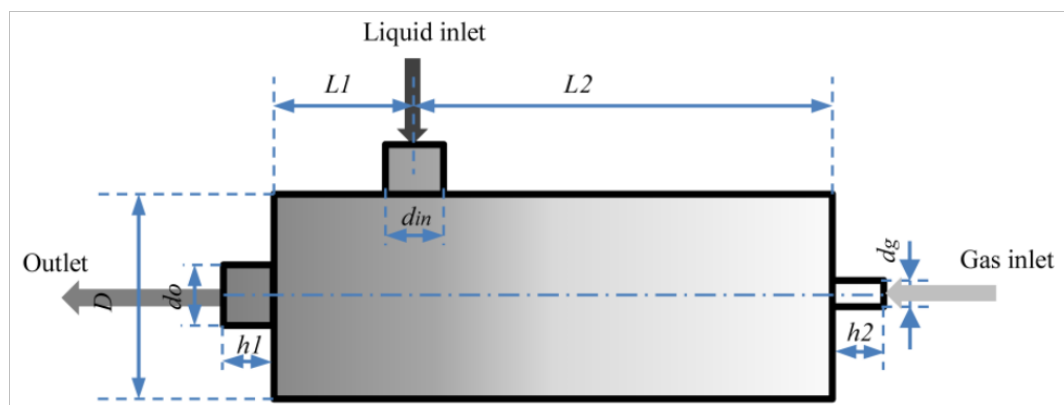


Figure 1.  
Schematic of MBG  
Swirl-Type [29]

The influence of gas inlet radius has been examined by Levitsky et al. [30], while Tabei et al. [2] investigated the impact of outlet channel radius, finding that a smaller outlet channel diameter results in smaller bubble diameters. Research on the effect of swirl chamber volume was conducted by Amini [31], revealing that reducing the swirl chamber area leads to an increase in axial velocity. On the other hand, Dhiputra and Wijayanta [32] studied nozzle dimensions using LPG gas vapor and observed that the discharge coefficient and Reynolds number are directly

proportional to the swirling chamber volume. The length of the swirling chamber was varied. However, to date, there has been no investigation into the influence of swirling chamber volume, especially by varying the length of the space, on the produced bubbles. The effect of swirling chamber length was elucidated by Sheen et al. [33], indicating that friction with the walls reduces axial and tangential momentum flux, a phenomenon referred to as swirl decay. This phenomenon was further explored by Fitzgerald et al. [34] and Carnevale et al. [35] using numerical methods.

In the subsequent study, tangential inlet water was employed to enter the swirling chamber, varying water and air flow rates [24]. Bubbles with a size of 150 microns were obtained by adjusting the water flow rate to 70 lpm and the air flow rate to 0.1 lpm. Likewise, Parmar and Majumder [36] and Tabei et al. [2] investigated the impact of varying inlet water pressure on the MBG. Their findings indicated that higher inlet pressure led to a significantly elevated swirl flow rotation number and increased flow velocity from the exit nozzle. The MBG in this scenario produced bubbles with an average diameter ranging from 40 to 70 microns. Additionally, Liao and Lucas [37] noted that an increase in water flow reduced bubble size due to heightened shear stress. Conversely, increasing air flow had the opposite effect, enlarging bubble size. Moving forward, Temesgen et al. [5] observed that an increase in water flow resulted in a decrease in the average diameter of formed bubbles and a more uniform bubble distribution. Conversely, an increase in air flow led to a rise in the average diameter of formed bubbles. Similar observations were made by other researchers [27], [28], [38]. Ohnari [28] emphasized the importance of optimal pump pressure for achieving higher microbubble concentrations, with air flow playing a crucial role in optimal bubble formation. In a related context, Kukizaki and Goto [39] highlighted that the swirl effect enhances fluid turbulence, increasing the instability of contact between bubbles and liquid, thereby reducing bubble size. Furthermore, Ohnari [28] suggested that a swirl MBG design, featuring an outlet channel protruding into the swirl space, can minimize kinetic energy loss and increase shear force, resulting in the production of smaller bubbles. The bubbles generated in this setup exhibited a diameter range of 50 - 200 nm. Rehman et al. [11] and Kukizaki and Goto [40] investigated a swirl MBG injecting helium gas into the generator containing mercury through a narrow gap. The generator, comprising a cylinder with vanes, facilitated the breakdown of gas into bubbles through the utilization of swirl flow.

Swirl flow in pipes is defined as a combination of vortex and axial movements with a spiral streamline [42]. Swirl flow, characterized by a non-zero tangential (azimuthal) velocity component, is always accompanied by an increase in velocity fluctuations. It represents a flow with a spiral motion on the tangential axis, in addition to the axial and radial directions [33]. There are several

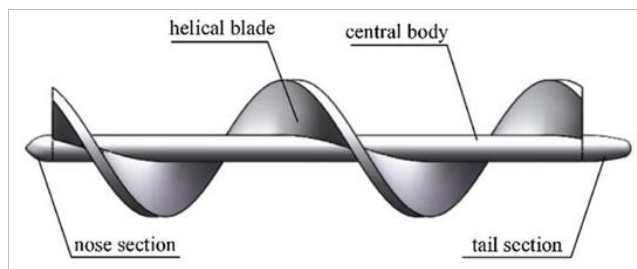


Figure 2.  
Twisted tape scheme  
[41]

methods for generating swirl [42], [43], such as using twisted tape, where tape inserts are attached to a shaft as illustrated in Figure 2 [4], [41], [44]–[46]; fixed-blade impellers attached to a shaft [33], [47]–[50]; rotating pipes [51], [52]; and tangential injection [2], [28]–[32], [53]–[56].

The swirl number, which can be employed to quantify the strength of swirl, is defined as the ratio of the azimuthal momentum flux to the axial momentum flux, expressed by Eq.(1) [42], where,  $\rho$  represents the fluid density. Then, Sinaga [43] stated that the increasing swirl number is directly proportional to the increase in velocity.

$$S_f(x) = \frac{2\pi\rho \int_0^R y^2 UV dy}{2\pi\rho R \int_0^R y U^2 dy} \quad (1)$$

At present, considerable attention is directed toward swirl bubble generators in both applied and research domains, with their performance emerging as a pivotal parameter. The size and distribution of bubbles stand as primary indices for assessing MBG efficacy. The profound interaction between gas and liquid is strategically employed within the mixing channel to yield a substantial quantity of bubbles. Given the escalating emphasis on swirl bubble generators, this discourse systematically reviews the advancements in fundamental research within this domain, facilitating a nuanced understanding applicable to optimal industrial implementation.

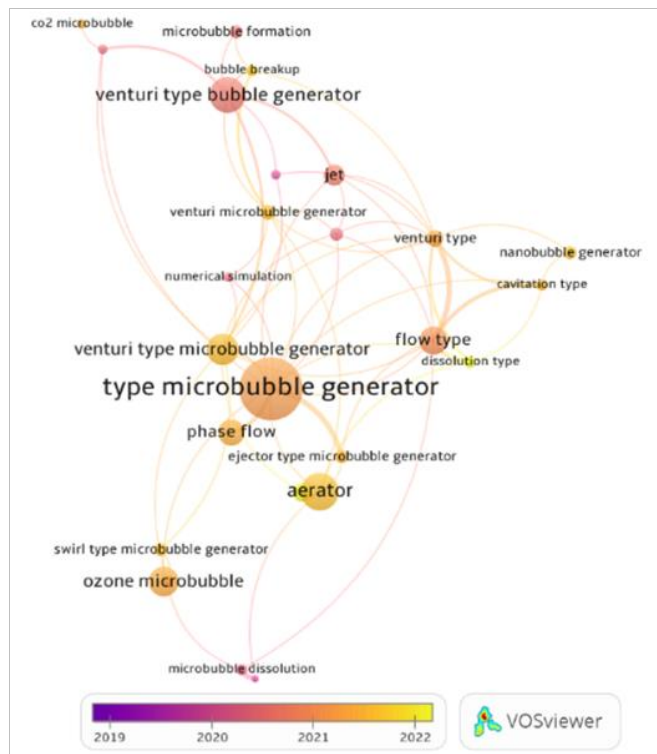


**Figure 3.** Trending research topics about microbubble generators generated by VOSviewer

Based on the results of the VOSviewer analysis, as seen in the overlay visualization presented in Figure 3, it depicts a mapping illustrating the degree of prevalence of research topics related to Swirl-type Microbubble Generators (MBG). The color of each node represents the publication time of the articles. Consequently, darker colors indicate that the research topic has been studied for a longer period, while lighter colors suggest that the research topic is relatively recent. As observed in the figure, research on the Microbubble Generator type is a relatively new field, spanning around 2020-2021. Studies specifically focusing on the Swirl-type Microbubble Generator are limited, as indicated by the smaller size of the nodes compared to research related to the Venturi-

type microbubble generator. Therefore, a comprehensive review manuscript on Swirl-type microbubble generators is highly warranted to advance research efforts and enrich the database about swirl-type microbubble generators.

## 2. Microbubble Generation Methods

MBGs are devices capable of producing microbubbles, and the methods for generating them are classified into three categories [36]. The first method involves the use of fluid flow. Some methods falling into this category include the spherical body in flowing tube, rotary liquid flow type, venturi [57]–[59]; rotary liquid flow type [60]; multifluid mixture device [3]; pressurize dissolution, ejector [25], [61], [62]; jet reactor [63]; and sparger [64], [65]. Fujikawa et al. [22] investigated a novel approach using a rotating porous plate to produce small bubbles. Meanwhile, [11] generated microbubbles using a fluid oscillator. The fluid oscillator can generate microbubbles with a diameter of 100  $\mu\text{m}$  by oscillating the gas flow to a pair of diffuser membranes. The fluid oscillator consists of two components: an amplifier and a feedback loop. The amplifier is fabricated using a CNC machine with acrylic glass plate material to form a specially designed cavity. The feedback loop connects the two control terminals of the amplifier. The second method involves the absence of fluid flow assistance. Some methods falling into this category include shirasu porous glass, porous membrane, electrolysis, vapor condensation system, and porous mullet ceramic technique [40]. Shirasu is volcanic ash containing core materials ( $\text{SiO}_2$  and  $\text{Al}_2\text{O}_3$ ) and impurity materials ( $\text{NaO}$ ,  $\text{K}_2\text{O}$ ,  $\text{CaO}$ ,  $\text{MgO}$ ,  $\text{Fe}_2\text{O}_3$ ). Meanwhile, the third method is the Low Power Generation Technique, which encompasses mechanical agitation and sonication [66]. Therefore, Table 1 presents the comparison of several MBGs produced by various researchers.

The swirl-type Microbubble Generator (MBG) is a bubble generation technology utilizing a tangential inlet method to induce rotational flow. In accordance with Bernoulli's law of energy conversion, as the liquid fluid passes through the tangential inlet channel located on one wall of the swirling chamber, it generates swirling flow. The increase in the ratio of angular momentum flux to axial momentum flux (swirl number) significantly enhances turbulence intensity, leading to reduced pressure at the center of the swirling water vortex. A sudden constriction event in the mixing channel causes water pressure to drop below atmospheric pressure, resulting in automatic air suction. The two phases mix within the mixing channel, forming a bubbly flow and subsequently creating secondary bubbles (ligaments), which undergo breakup due to sudden enlargement at the MBG outlet [24].

**Table 1.**  
Comparison of  
microbubble generator

MBG types and refs.	Usage Recommendations	Advantages	Disadvantages
Injector [67]	-	<ul style="list-style-type: none"> <li>Simple construction.</li> <li>Does not require a compressor to deliver air.</li> </ul>	Air supply through the pump's suction side can lead to cavitation in the pump.
Porous [68]	Clean water and wastewater	Does not require a compressor to deliver air.	The size of the generated microbubbles is influenced by fluid velocity and pore diameter.
High shear [68]	Clean water and wastewater	Does not require a pump to generate microbubbles.	It requires electrical power to drive the blade used for bubble fragmentation.
Inline [68]	Clean water	Air supply does not need to be pressurized.	The process of manufacturing and installing the blade (vane) is quite challenging.
Spherical body [38]	Clean water	<ul style="list-style-type: none"> <li>Does not require a compressor to deliver air.</li> <li>Can produce bubbles with a diameter of 0.12 mm.</li> </ul>	<ul style="list-style-type: none"> <li>The size of the generated microbubbles is affected by water and air flow rates.</li> <li>The placement of the spherical body affects bubble size.</li> <li>The gap between the sphere and the channel is very narrow, posing a high risk of blockage if the flowing water contains impurities.</li> </ul>
Shirasu porous glass [39]	Clean water	Capable of producing bubbles with a diameter of 360-720 nm.	<ul style="list-style-type: none"> <li>Pressurized air supply is achieved using a compressor.</li> <li>The study is conducted employing a surfactant, with no information provided regarding its use in pure water.</li> </ul>
Swirl jet [2]	Clean water and wastewater	<ul style="list-style-type: none"> <li>Simple construction.</li> <li>Frequently occurring bubble diameter ranges between 40 <math>\mu\text{m}</math> and 70 <math>\mu\text{m}</math>.</li> </ul>	<ul style="list-style-type: none"> <li>Sufficient fluid velocity at the outlet is necessary for the bubble formation process.</li> <li>The size of the generated microbubbles is influenced by the fluid and air flow rates.</li> </ul>
Venturi structure [18], [69]	Clean water dan wastewater	<ul style="list-style-type: none"> <li>Simple construction.</li> <li>Average produced bubble diameter is 50 <math>\mu\text{m}</math>.</li> </ul>	The size of the generated microbubbles is influenced by the water and air flow rates.
Multi fluid mixture with orifice [3]	Clean water dan wastewater	<ul style="list-style-type: none"> <li>Does not require a compressor for air flow.</li> <li>Can generate bubbles with a diameter of 0.01-0.05 mm.</li> </ul>	The size of the generated microbubbles is influenced by the fluid and air flow rates.
Porous membrane [70]	Clean water	The porous media structure results in shear stress changes in the fluid having no significant effect on bubble diameter changes.	Pressurized air supply is employed due to the very small pore diameter (0.8 and 0.1 $\mu\text{m}$ ).
Porous orifice-type MBG [6]	Clean water	<ul style="list-style-type: none"> <li>Simple construction.</li> <li>Average produced bubble diameter is 200 <math>\mu\text{m}</math>.</li> </ul>	The size of the generated microbubbles is influenced by the fluid and air flow rates.
Swirl-type MBG [24]	Clean water	<ul style="list-style-type: none"> <li>Simple construction.</li> <li>Average produced bubble diameter is 150 <math>\mu\text{m}</math>.</li> </ul>	The size of the generated microbubbles is influenced by the fluid and air flow rates.

### 3. Discussion

#### 3.1. MBG Performance

The performance of the Microbubble Generator (MBG) can be determined based on the diameter and distribution of the generated bubbles [2], [23], [71], [72]. Small bubble diameters result in a decrease in bubble rise velocity, a characteristic that allows bubbles to persist for an extended period in water. Meanwhile, the distribution of bubble sizes influences the gas-liquid

contact area, gas holdup, and bubble rising velocity [3], [71], [72]. These parameters serve as references in designing an efficient MBG [23].

The smaller the diameter of the bubbles, the larger their surface area [10], [23]. Surface area significantly influences mass transfer performance [25], a crucial factor in various applications such as distillation, absorption/desorption, and multiphase agitation [10], [73]. High mass transfer coefficients and interfacial areas can reduce the size of mass transfer contactors significantly, thereby minimizing operational costs in water treatment processes [74]. In flotation and aeration processes, smaller bubbles have been proven to be more effective in capturing flocs and facilitating gas transfer [71]. Gas holdup is a crucial parameter for characterizing mixing and mass transfer between gas and liquid. Gas holdup ( $\epsilon_G$ ) is the volume fraction occupied by bubbles or gas, defined by Eq (2) [7], [75], [76]. Where,  $V_G$  represents the volume occupied by the gas phase, while  $V_L$  denotes the volume occupied by the liquid phase.

$$\epsilon_G = \frac{V_G}{V_L + V_G} \quad (2)$$

In general, gas holdup is crucial for determining the interfacial area per unit volume and is thus utilized to assess the efficiency of MBG [13], [66]. Gas holdup determines the quantity of floating material that can adhere to the gas phase [65]. In MBGs functioning as photobioreactors to enhance microalgae growth, gas holdup can serve as an indicator of solubility and bubble residence [9]. Gas holdup can be measured using various methods [25], [59] including the differential pressure method, volume expansion method, and X-ray tomography. The measurement method for holdup formulated by Amagai [75] involves a constant flow carried through a liquid flow pipe with a DC power supply.

Dissolved Oxygen (DO) serves as a crucial parameter to assess the performance of microbubble generators concerning the enhancement of dissolved oxygen levels in water. Microbubbles facilitate a quicker dissolution of oxygen [12], [13]. DO is also employed as a performance parameter for MBG in applications aimed at enhancing microorganism productivity [13], [77]. Agarwal et al. [7] assert that air and nitrogen in the form of microbubbles and nanobubbles can enhance the activities of aerobic and anaerobic microorganisms. DO is significantly influenced by the size and distribution of bubbles generated by MBG [3], [6], [38]. The low bubble rise velocity allows bubbles to persist in water for an extended period [23], thereby improving mass transfer, which can enhance aeration performance [6], [72].

### 3.2. Methods for Investigating MBG Performance

The methods employed to investigate the performance of microbubbles have been extensively pursued by previous researchers. Generally, the methodologies are designed to acquire data on bubble size along with its distribution. Bubble sizes are predominantly measured through images captured using a high-speed camera [2], [6], [24]. Subsequently, the images are processed using algorithms to identify bubbles within the water [23] and determine their sizes. The image analysis algorithm is outlined by Lau et al. [78] and comprises four main operations:

1. Image filtering. Firstly, the correction of inhomogeneous background illumination is performed using thresholding. Secondly, an edge detection algorithm is employed to enhance the distinction between bubbles and the background. Thirdly, the image is converted into a binary image, and noise is subsequently eliminated.
2. The separation of bubble objects into single bubbles and overlapping bubbles is conducted using the roundness level. If  $R_o < 1.25$ , it is classified as a single bubble.
3. The utilization of the water-shedding technique to segment overlapping bubbles. The water-shedding technique is processed as follows: inverting the contrast color of the image to enhance the brightness of bubbles compared to the background; detecting the area within bubbles due to their distinct color intensity from the background in grayscale images; applying thresholding to the image to identify the number of overlapping bubbles; marking the identified bubbles according to local minima; and recognizing overlapped bubbles as distinct individual entities.
4. Combining single bubbles with separated overlapping bubbles.

This method was subsequently refined by Juwana et al. [6] employing a roundness ratio ( $R_o$ ) of  $< 1.1$  for individual bubbles and  $> 1.1$  for overlapping conical bubbles.

The development of image processing based on MATLAB code, aimed at recognizing gas and liquid interfaces while simultaneously eliminating noise, was conducted by Liu et al. [79]. The steps undertaken are as follows:

1. Obtaining images for image processing using a high-speed camera.
2. Highlighting the effective regions of the image to reduce computational load.
3. Filtering and enhancing contrast. The median filter (`medfilt2` function) with a sliding window (3x3) is applied to reduce the impact of pixel-level noise, and histogram adjustment (`imadjust` function) is used to enhance image contrast.
4. Binarizing the image is converted from grayscale to binary mode using Otsu's method. The optimal threshold for distinguishing between gas and liquid interfaces is identified using the `graythresh` function. Once the threshold value is determined, a binary image is obtained using `im2bw`.
5. Filling bright 'holes.' Due to uneven brightness in the source image, the gas core regions may not be entirely dark in the binary image. To address this, the `imfill` and `imcomplement` functions are employed to define bright 'holes' in the gas core areas.

The similar method has also been employed by Swart et al. [72] and Bao et al. [73], incorporating edge detection processes. To determine the frequency of bubble occurrence at specific sizes or probability density function [2], [6], [23]–[25], [80]. Kress and Keyes [81] employed a Polaroid camera and strobe flash lamp to measure bubble diameter. To investigate bubble distribution, the LTM-BSizer technique was employed [82], Particle Tracking Velocimetry (PTV) was utilized [83], simulations were conducted using a Multifase Compact Cyclonic Separator [54], such as the Gas-Liquid Cylindrical Cyclone (GLCC), which operates based on the centrifugal force generated by the rotating two-phase flow, the Malvern RTsizer was employed [79], a pressure drop-based measuring device was used to accurately monitor flow rates and fluid densities in a mixture of foamy air, water, and ethanol [84]. The Dynamic Exhaust method was employed to measure mass transfer coefficients [85]. The volumetric expansion method was used to determine gas holdup by measuring the solubility difference with bubbles in the solution.

### 3.3. Numerical Method

In addition to employing experimental methods, the investigation of Microbubble Generators (MBG) performance has also been pursued through numerical techniques. Wang et al. [86] utilized a two-fluid numerical calculation approach to investigate one-dimensional bubbly flow through a converging-diverging nozzle. The equation model assumes gas bubbles within the liquid, assuming them to be spherical and monodispersed across all cross-sections. Mass transfer, turbulence, bubble coalescence, and fission are neglected. The liquid phase is treated as incompressible and uniform in temperature. The effect of viscosity on pressure gradients in the liquid is modeled using a wall friction model. The two-phase mixture employs the average momentum equation. Inertia effects related to bubble growth and destruction are calculated using the Rayleigh-Plesset equation. Effective viscosity is utilized to model the damping of bubble motion in the radial direction. Liu and Bai [87] modeled a steady, incompressible 3D gas-liquid flow, Luo et al. [41] utilizing the ANSYS numerical simulation method to simulate the continuous flow of gas. The employed model is a multiphase mixture consisting of continuity and momentum equations. Turbulence modeling for swirling flow utilized the RNG  $k$ - $\epsilon$  model. Meanwhile, Sun et al. [88] performed simulations for Venturi-type Microbubble Generator (MBG) in the context of a Thorium Molten Salt Reactor (TMSR) using CFD FLUENT. The algorithm employed was SIMPLE, involving pressure, momentum, turbulent kinetic energy, turbulent dissipation rate, and Reynolds stress in second order. The simulation employed the  $k$ - $\epsilon$  turbulence model due to its ability to produce high pressure drops in low-flow-rate water scenarios.

The simulations conducted by Sharma et al. [61] and Alam et al. [26] employed the Reynolds-Averaged Navier-Stokes (RANS) equations to model swirl flow. The turbulence model employed the  $k$ - $\epsilon$  equations, including momentum, continuity, and energy conservation equations. The meshing process utilized tetrahedral elements with boundary conditions set as follows: gas inlet pressure at one atmosphere and liquid inlet flow rate at 50 l/min.

The CFD simulation method using ANSYS CFX was formulated by Alam et al. [89] involving the modeling of swirl flow through the Reynolds-Averaged Navier-Stokes (RANS) equations and employing conservation equations to model multiphase flow. Particle Image Velocimetry (PIV) measurements were conducted to determine microbubble velocity, as Basso et al. [90] utilized the Discrete Phase Model (DPM) combined with the Rosin-Rammler method to simulate air bubbles in the form of dispersed particles in water. Meanwhile, Huang et al. [91] utilized the ANSYS-ICEM software to generate both structured and unstructured meshes. Unstructured meshes were produced to ensure sufficient adaptation to the complexity of the geometry. Vortex evolution was observed by Kudela and Kosior [92] using paint particles through numerical simulation. Typically,

the observation of vortex evolution employs paint particles. However, in viscous fluids, paint particles may not accurately track vortex evolution, necessitating the use of numerical methods for observation.

### 3.4. Mechanism of Bubble Formation from Swirling Flow

The mechanism of bubble breakup occurs because of the balance between the external pressure from the liquid phase attempting to break up the bubble and the surface tension of the bubble tending to restore its shape. The breakup mechanism is categorized into four main categories: (a) turbulent fluctuations and collisions; (b) viscous shear stress; (c) separation processes due to shear stress; and (d) surface instability [37]. In swirl-type Microbubble Generators (MBG) employing tangential inlets, the variation in swirling velocity results in increased shear stress. This shear stress is utilized to break down the bubbles into smaller sizes [2], [26], [30], [53]. Forces such as friction, lift, additional mass, and turbulent dispersion on the MBG will significantly influence the movement, deformation, and breakup of moving bubbles [59], [93].

Kuo and Wallis [93] developed a balance model for bubbly flow in the nozzle, Lasheras et al. [80] conducted a study on the breakup frequency of bubbles under highly controlled turbulent conditions. Meanwhile, Wilkinson et al. [94] conducted experiments using turbulent flow in both vertical and horizontal pipes. Single bubbles were manually injected using a syringe for easy observation. The fluid flow velocity near the injection point was kept low to prevent bubble destruction. Flow circulation speed was controlled using valves and a flowmeter. Optical instrumentation with a high-speed film at 5000 fps was utilized to determine the number of bubble fragments. In horizontal pipes, bubbles tended to approach the upper wall due to buoyancy forces directed towards the wall, resulting in the highest shear force. The higher the bubble density and the larger the bubble diameter, the greater the likelihood of bubble destruction. Longer pipes led to more bubble destruction due to prolonged turbulence. Breakup of bubbles in turbulent flow commonly occurred due to the loss of small bubbles in the vicinity of the pipe wall. In our previous study [24], The bubble burst mechanism was visually found at a water flow rate of 30 lpm and an air flow rate of 0.1 lpm. When fluid flows through a suddenly expanded cross-section, there is a sudden change in flow velocity from high to low, leading to the formation of bubbly flow along the mixing channel. This results in the formation of a ligament in the MBG(a) exit channel. Subsequently, due to changes in pressure difference, this movement undergoes breakup, forming small bubbles (b). The bubble sizes are then separated by the rotating flow (c), as illustrated in Figure 4. After experiencing the breakup event, where small-sized bubbles move away from the axis of rotation and large-sized bubbles move towards the axis of rotation, the subsequent flow separates the bubbles with a rotational motion. Due to pressure changes, the rotational flow propagates away from the MBG outlet.

## 4. Conclusion

The Swirl-type bubble generator is one of the promising methods for producing fine bubbles, thus motivating researchers to conduct extensive experimental and theoretical studies. This paper reviews published papers on recent developments in research on Swirl-type bubble generators, including definitions of microbubbles, methods of microbubble generation through experimental and numerical approaches, microbubble generator performance, and its applications. The following conclusions can be drawn:

1. Microbubbles are micron-sized bubbles characterized by a size scale ranging between micrometers and millimeters in diameter.
2. The swirl-type microbubble generator can produce small-sized bubbles more effectively compared to other types, with broad applications. The bubble breakup phenomenon in swirl-type microbubble generators begins with the formation of bubble channels in the mixing channel, followed by ligament formation at the outlet side of the microbubble generator (MBG), leading to the subsequent breakup into small-sized bubbles.
3. The probability distribution of the generated bubble sizes and their mean diameter are key parameters reflecting the performance of the Swirl-type bubble generator. This performance is highly dependent on flow conditions (gas and liquid flow rates) and geometric configurations. Particularly, the ratio between air and water velocities within the microbubble generator and the turbulence force of the flow are crucial factors. The precise combination of flow conditions and geometric configurations will yield well-controlled bubble sizes suitable for practical applications.

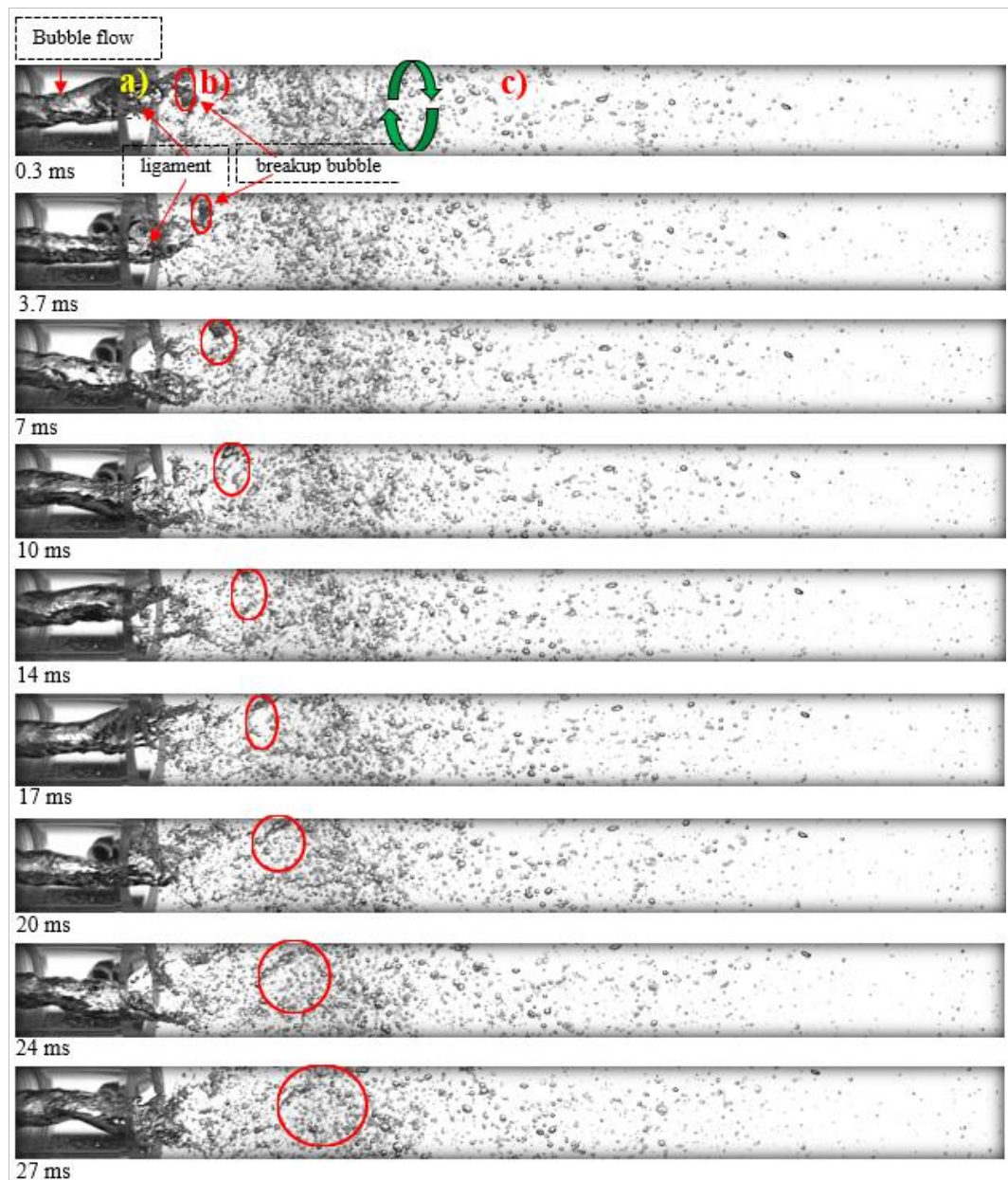


**Figure 4.**  
Mechanism of bubble  
breakup in Swirl-type  
MBG [24]

## Authors' Declaration

**Authors' contributions and responsibilities** - The authors made substantial contributions to the conception and design of the study.

**Funding** – No funding information from the authors.

**Availability of data and materials** - All data is available from the authors.

**Competing interests** - The authors declare no competing interest.

**Additional information** – No additional information from the authors.

## References

- [1] G. P. Galdi, *Particles in Flows*, 1st ed. Birkhäuser Cham, 2014.
- [2] F. T. Katsuine Tabei, Shuka Haruyama, Shuichi Yamaguchi, Hiroyuki Shirai, "Study of Micro Bubble Generation by a Swirl Jet (Measurement of Bubble Distribution by Light Transmission and Characteristics of Generation Bubbles)," *Journal of Environment and Engineering*, vol. 2, no. 1, pp. 172–182, 2007, doi: 10.1299/jee.2.172.
- [3] M. Sadatomi, A. Kawahara, H. Matsuura, and S. Shikatani, "Micro-bubble generation rate and

- bubble dissolution rate into water by a simple multi-fluid mixer with orifice and porous tube," *Experimental Thermal and Fluid Science*, vol. 41, pp. 23–30, 2012, doi: 10.1016/j.expthermflusci.2012.03.002.
- [4] W. Liu and B. Bai, "Two-phase flow patterns and pressure drop inside a vertical pipe containing a short helical tape insert," *American Society of Mechanical Engineers, Fluids Engineering Division (Publication) FEDSM*, vol. 1D, pp. 1–9, 2014, doi: 10.1115/FEDSM2014-21144.
- [5] T. Temesgen, T. T. Bui, M. Han, T. il Kim, and H. Park, "Micro and nanobubble technologies as a new horizon for water-treatment techniques: A review," *Advances in Colloid and Interface Science*, vol. 246, pp. 40–51, 2017, doi: 10.1016/j.cis.2017.06.011.
- [6] W. E. Juwana, A. Widyatama, O. Dinaryanto, W. Budhijanto, Indarto, and Deendarlianto, "Hydrodynamic characteristics of the microbubble dissolution in liquid using orifice type microbubble generator," *Chemical Engineering Research and Design*, vol. 141, pp. 436–448, 2019, doi: 10.1016/j.cherd.2018.11.017.
- [7] A. Agarwal, W. J. Ng, and Y. Liu, "Principle and applications of microbubble and nanobubble technology for water treatment," *Chemosphere*, vol. 84, no. 9, pp. 1175–1180, 2011, doi: 10.1016/j.chemosphere.2011.05.054.
- [8] W. Zhang, M. Rezaee, A. Bhagavatula, Y. Li, J. Groppo, and R. Honaker, "A review of the occurrence and promising recovery methods of rare earth elements from coal and coal by-products," *International Journal of Coal Preparation and Utilization*, vol. 35, no. 6, pp. 295–330, 2015, doi: 10.1080/19392699.2015.1033097.
- [9] J. Cheng *et al.*, "Bioresource Technology A novel jet-aerated tangential swirling-flow plate photobioreactor generates microbubbles that enhance mass transfer and improve microalgal growth," *Bioresource Technology*, vol. 288, no. May, p. 121531, 2019, doi: 10.1016/j.biortech.2019.121531.
- [10] A. Yoshida, O. Takahashi, Y. Ishii, Y. Sekimoto, and Y. Kurata, "Water purification using the adsorption characteristics of microbubbles," *Japanese Journal of Applied Physics, Part 1: Regular Papers and Short Notes and Review Papers*, vol. 47, no. 8 PART 1, pp. 6574–6577, 2008, doi: 10.1143/JJAP.47.6574.
- [11] F. Rehman, G. J. D. Medley, H. Bandulasena, and W. B. J. Zimmerman, "Fluidic oscillator-mediated microbubble generation to provide cost effective mass transfer and mixing efficiency to the wastewater treatment plants," *Environmental Research*, vol. 137, pp. 32–39, 2015, doi: 10.1016/j.envres.2014.11.017.
- [12] L. Marbelia *et al.*, "A Comparative Study of Conventional Aerator and Microbubble Generator in Aerobic Reactors for Wastewater Treatment," *IOP Conference Series: Materials Science and Engineering*, vol. 778, no. 1, 2020, doi: 10.1088/1757-899X/778/1/012132.
- [13] K. Terasaka, A. Hirabayashi, T. Nishino, S. Fujioka, and D. Kobayashi, "Development of microbubble aerator for waste water treatment using aerobic activated sludge," *Chemical Engineering Science*, vol. 66, no. 14, pp. 3172–3179, 2011, doi: 10.1016/j.ces.2011.02.043.
- [14] H. Zhou and D. W. Smith, "Ozone mass transfer in water and wastewater treatment: Experimental observations using a 2D laser particle dynamics analyzer," *Water Research*, vol. 34, no. 3, pp. 909–921, 2000, doi: 10.1016/S0043-1354(99)00196-7.
- [15] J. Zhu *et al.*, "Cleaning with Bulk Nanobubbles," *Langmuir*, vol. 32, no. 43, pp. 11203–11211, 2016, doi: 10.1021/acs.langmuir.6b01004.
- [16] S. Liu, Q. Wang, H. Ma, P. Huang, J. Li, and T. Kikuchi, "Effect of micro-bubbles on coagulation flotation process of dyeing wastewater," *Separation and Purification Technology*, vol. 71, no. 3, pp. 337–346, 2010, doi: 10.1016/j.seppur.2009.12.021.
- [17] P. E. Poh, W. Y. J. Ong, E. V. Lau, and M. N. Chong, "Investigation on micro-bubble flotation and coagulation for the treatment of anaerobically treated palm oil mill effluent (POME)," *Journal of Environmental Chemical Engineering*, vol. 2, no. 2, pp. 1174–1181, 2014, doi: 10.1016/j.jece.2014.04.018.
- [18] M. Ishikawa, K. Irbabu, I. Teruya, and M. Nitta, "PIV measurement of a contraction flow using micro-bubble tracer," *Journal of Physics: Conference Series*, vol. 147, pp. 0–5, 2009, doi: 10.1088/1742-6596/147/1/012010.
- [19] M. Kogawa, H., Naoe, T., Kyotoh, H., Haga, K., Kinoshita, H., Futakawa., "Development of

- Microbubble Generator for Suppression of Pressure Wave in Mercury Target of Spallation Source,” *Journal of Nuclear Science and Technology*, vol. 52, no. 12, 2015.
- [20] C. Barbier, E. Dominguez-Ontiveros, and R. Sangrey, “Small bubbles generation with swirl bubblers for SNS target,” *American Society of Mechanical Engineers, Fluids Engineering Division (Publication) FEDSM*, vol. 3, 2018, doi: 10.1115/FEDSM2018-83077.
- [21] I Ketut Daging, Pungkas Prayitno, Iwan G. Wardana, Akhmad Syarifudin, Hendro Sukismo, and Sugianto, “Rancang Bangun Alat Aerasi Mikro Bubblepada Budidaya Air Tawar,” *Journal of Innovation Research and Knowledge*, vol. 2, no. 1, pp. 239–244, 2022.
- [22] S. Fujikawa, R. Zhang, S. Hayama, and G. Peng, “The control of micro-air-bubble generation by a rotational porous plate,” *International Journal of Multiphase Flow*, vol. 29, no. 8, pp. 1221–1236, 2003, doi: 10.1016/S0301-9322(03)00106-X.
- [23] A. Gordiychuk, M. Svanera, S. Benini, and P. Poesio, “Size distribution and Sauter mean diameter of micro bubbles for a Venturi type bubble generator,” *Experimental Thermal and Fluid Science*, vol. 70, pp. 51–60, 2016, doi: 10.1016/j.expthermflusci.2015.08.014.
- [24] D. I. Mawarni, W. E. Juwana, K. A. Yuana, W. Budhijanto, Deendarlianto, and Indarto, “Hydrodynamic characteristics of the microbubble dissolution in liquid using the swirl flow type of microbubble generator,” *Journal of Water Process Engineering*, vol. 48, no. 2, p. 102846, 2022, doi: 10.1016/j.jwpe.2022.102846.
- [25] X. Wang et al., “Bubble breakup in a swirl-venturi microbubble generator,” *Chemical Engineering Journal*, vol. 401, no. January, 2021, doi: 10.1016/j.cej.2020.126397.
- [26] H. S. Alam, Bahrudin, A. T. Sugiarto, and G. G. Redhyka, “Unsteady numerical simulation of gas-liquid flow in dual chamber microbubble generator,” in *Proceedings of the 2nd International Conference on Automation, Cognitive Science, Optics, Micro Electro-Mechanical System, and Information Technology, ICACOMIT 2017*, 2017, vol. 2018-Janua, no. 1, pp. 133–137, doi: 10.1109/ICACOMIT.2017.8253401.
- [27] M. L. Jackson, “Aeration in Bernoulli types of devices,” *AIChE Journal*, vol. 10, no. 6, pp. 836–842, 1964, doi: 10.1002/aic.690100612.
- [28] H. Ohnari, “Swirling Fine-Bubble Generator,” US638260B1, 2002.
- [29] X. Xu, X. Ge, Y. Qian, B. Zhang, H. Wang, and Q. Yang, “Effect of nozzle diameter on bubble generation with gas self-suction through swirling flow,” *Chemical Engineering Research and Design*, vol. 138, pp. 13–20, 2018, doi: 10.1016/j.cherd.2018.04.027.
- [30] I. Levitsky, V. Gitis, and D. Tavor, “Generation of Coarse Bubbles and Flow Instability Control by Means of a Bubble Generator,” *Chemical Engineering and Technology*, vol. 42, no. 5, pp. 1127–1134, 2019, doi: 10.1002/ceat.201800158.
- [31] G. Amini, “Liquid flow in a simplex swirl nozzle,” *International Journal of Multiphase Flow*, vol. 79, pp. 225–235, 2016, doi: 10.1016/j.ijmultiphaseflow.2015.09.004.
- [32] H. I. M. K. Dhiputra and S. Wijayanta, “Discharge coefficient of swirling nozzle with swirling chamber volume variation for liquefied petroleum gas,” *World Applied Sciences Journal*, vol. 25, no. 3, pp. 369–376, 2013, doi: 10.5829/idosi.wasj.2013.25.03.2691.
- [33] H. J. Sheen, W. J. Chen, S. Y. Jeng, and T. L. Huang, “Correlation of Swirl Number for a Radial-Type Swirl Generator,” *Experimental Thermal and Fluid Science*, vol. 12, no. 4, pp. 444–451, 1996, doi: 10.1016/0894-1777(95)00135-2.
- [34] A. J. Fitzgerald, K. Hourigan, and M. C. Thompson, “Vortex breakdown state selection as a meta-stable process,” *ANZIAM Journal*, vol. 46, p. 351, 2005, doi: 10.21914/anziamj.v46i0.964.
- [35] G. F. Carnevale, R. C. Kloosterziel, P. Orlandi, and D. D. J. A. Van Sommeren, “Predicting the aftermath of vortex breakup in rotating flow,” *Journal of Fluid Mechanics*, vol. 669, no. May 2014, pp. 90–119, 2011, doi: 10.1017/S0022112010004945.
- [36] R. Parmar and S. K. Majumder, “Microbubble generation and microbubble-aided transport process intensification-A state-of-the-art report,” *Chemical Engineering and Processing: Process Intensification*, vol. 64, pp. 79–97, 2013, doi: 10.1016/j.cep.2012.12.002.
- [37] Y. Liao and D. Lucas, “A literature review of theoretical models for drop and bubble breakup in turbulent dispersions,” *Chemical Engineering Science*, vol. 64, no. 15, pp. 3389–3406, 2009, doi: 10.1016/j.ces.2009.04.026.
- [38] A. Sadatomi, M., Kawahara, A., Kano, K., and Ohtomo, “Performance of New Micro-Bubble

- Generator With A Spherical Body in Flowing Water Tube,” *Experimental Thermal and Fluid Science*, vol. 29, pp. 615–623, 2005.
- [39] M. Kukizaki and M. Goto, “Size control of nanobubbles generated from Shirasu-porous-glass (SPG) membranes,” *Journal of Membrane Science*, vol. 281, no. 1–2, pp. 386–396, 2006, doi: 10.1016/j.memsci.2006.04.007.
- [40] M. Kukizaki and M. Goto, “Spontaneous formation behavior of uniform-sized microbubbles from Shirasu porous glass (SPG) membranes in the absence of water-phase flow,” *Colloids and Surfaces A: Physicochemical and Engineering Aspects*, vol. 296, no. 1–3, pp. 174–181, 2007, doi: 10.1016/j.colsurfa.2006.09.042.
- [41] X. Luo, L. Yang, H. Yin, L. He, and Y. Lü, “A review of vortex tools toward liquid unloading for the oil and gas industry,” *Chemical Engineering and Processing - Process Intensification*, vol. 145, no. October, p. 107679, 2019, doi: 10.1016/j.cep.2019.107679.
- [42] A. Islek, “The Impact of Swirl in Turbulent Pipe Flow,” Georgia Institute of Technology, 2004.
- [43] N. Sinaga, “Kaji Numerik Aliran Jet-Swirling Pada Saluran Annulus Menggunakan Metode Volume Hingga,” *Rotasi*, vol. 19, no. 2, p. 52, 2017, doi: 10.14710/rotasi.19.2.52-60.
- [44] C. H. Lee, H. Choi, D. W. Jerng, D. E. Kim, S. Wongwises, and H. S. Ahn, “Experimental investigation of microbubble generation in the venturi nozzle,” *International Journal of Heat and Mass Transfer*, vol. 136, pp. 1127–1138, 2019, doi: 10.1016/j.ijheatmasstransfer.2019.03.040.
- [45] F. T. Kanizawa and G. Ribatski, “Two-phase flow patterns and pressure drop inside horizontal tubes containing twisted-tape inserts,” *International Journal of Multiphase Flow*, vol. 47, pp. 50–65, 2012, doi: 10.1016/j.ijmultiphaseflow.2012.07.003.
- [46] Z. Qiao, Z. Wang, C. Zhang, S. Yuan, Y. Zhu, and J. Wang, “PVAm–PIP/PS composite membrane with high performance for CO<sub>2</sub>/N<sub>2</sub> separation,” *AIChE Journal*, vol. 59, no. 4, pp. 215–228, 2012, doi: 10.1002/aic.13781.
- [47] H. Funahashi, K. Hayashi, S. Hosokawa, and A. Tomiyama, “Two-phase swirling flow in a gas-liquid separator,” *Transactions of the American Nuclear Society*, vol. 113, no. 4, pp. 1454–1455, 2015, doi: 10.1299/jpes.2.1120.
- [48] F. Liang, J. Chen, J. Wang, H. Yu, and X. Cao, “Gas-liquid two-phase flow equal division using a swirling flow distributor,” *Experimental Thermal and Fluid Science*, vol. 59, pp. 43–50, 2014, doi: 10.1016/j.expthermflusci.2014.07.013.
- [49] L. Liu and B. Bai, “Flow regime identification of swirling gas-liquid flow with image processing technique and neural networks,” *Chemical Engineering Science*, vol. 199, pp. 588–601, 2019, doi: 10.1016/j.ces.2019.01.037.
- [50] Y. Yang, D. Wang, P. Niu, M. Liu, and S. Wang, “Gas-liquid two-phase flow measurements by the electromagnetic flowmeter combined with a phase-isolation method,” *Flow Measurement and Instrumentation*, vol. 60, pp. 78–87, 2018, doi: 10.1016/j.flowmeasinst.2018.02.002.
- [51] S. Imao, M. Itoh, and T. Harada, “Turbulent characteristics of the flow in an axially rotating pipe,” *International Journal of Heat and Fluid Flow*, vol. 17, no. 5, pp. 444–451, 1996, doi: 10.1016/0142-727X(96)00057-4.
- [52] H. Yamaguchi, D. Matsubara, and S. Shuchi, “Flow characteristics and micro-bubble behaviour in a rotating pipe section with an abrupt enlargement,” *Proceedings of the Institution of Mechanical Engineers, Part C: Journal of Mechanical Engineering Science*, vol. 215, no. 12, pp. 1447–1457, 2001, doi: 10.1243/0954406011524801.
- [53] P. Srinoi and K. Sato, “Controllable Air-bubbles Size Generator Performance with Swirl Flow,” *KMUTNB International Journal of Applied Science and Technology*, vol. 8, no. 4, pp. 1–5, 2015, doi: 10.14416/j.ijast.2015.08.002.
- [54] L. Gomez, R. Mohan, and O. Shoham, “Swirling gas-liquid two-phase flow - Experiment and modeling part II: Turbulent quantities and core stability,” *Journal of Fluids Engineering, Transactions of the ASME*, vol. 126, no. 6, pp. 943–959, 2004, doi: 10.1115/1.1849254.
- [55] R. Hreiz, R. Lainé, J. Wu, C. Lemaitre, C. Gentric, and D. Fünfschilling, “On the effect of the nozzle design on the performances of gas-liquid cylindrical cyclone separators,” *International Journal of Multiphase Flow*, vol. 58, pp. 15–26, 2014, doi: 10.1016/j.ijmultiphaseflow.2013.08.006.

- [56] Y. Hato, "Micro-bubble generator and micro-bubble generation device," US008991796B2, 2015.
- [57] J. Huang *et al.*, "A review on bubble generation and transportation in Venturi-type bubble generators," *Experimental and Computational Multiphase Flow*, vol. 2, no. 3, pp. 123–134, 2020, doi: 10.1007/s42757-019-0049-3.
- [58] L. Zhao *et al.*, "Effects of the divergent angle on bubble transportation in a rectangular Venturi channel and its performance in producing fine bubbles," *International Journal of Multiphase Flow*, vol. 114, pp. 192–206, 2019, doi: 10.1016/j.ijmultiphaseflow.2019.02.003.
- [59] S. I. Uesawa, A. Kaneko, Y. Nomura, and Y. Abe, "Fluctuation of void fraction in the microbubble generator with a venturi tube," *ASME-JSME-KSME 2011 Joint Fluids Engineering Conference, AJK 2011*, vol. 1, no. PARTS A, B, C, D, pp. 2483–2492, 2011, doi: 10.1115/AJK2011-10014.
- [60] R. Etchepare, H. Oliveira, M. Nicknig, A. Azevedo, and J. Rubio, "Nanobubbles: Generation using a multiphase pump, properties and features in flotation," *Minerals Engineering*, vol. 112, no. March, pp. 19–26, 2017, doi: 10.1016/j.mineng.2017.06.020.
- [61] D. Sharma, A. Patwardhan, and V. Ranade, "Effect of turbulent dispersion on hydrodynamic characteristics in a liquid jet ejector," *Energy*, vol. 164, pp. 10–20, 2018, doi: 10.1016/j.energy.2018.08.171.
- [62] J. Zahradník, M. Fialová, V. Linek, J. Sinkule, J. Řezníčková, and F. Kaštánek, "Dispersion efficiency of ejector-type gas distributors in different operating modes," *Chemical Engineering Science*, vol. 52, no. 24, pp. 4499–4510, 1997, doi: 10.1016/S0009-2509(97)00294-7.
- [63] Y. Shuai *et al.*, "Bubble Size Distribution and Rise Velocity in a Jet Bubbling Reactor," *Industrial and Engineering Chemistry Research*, vol. 58, no. 41, pp. 19271–19279, 2019, doi: 10.1021/acs.iecr.9b03880.
- [64] S. K. Pallapothu and A. M. Al Taweel, "Effect of contaminants on the gas holdup and mixing in internal airlift reactors equipped with microbubble generator," *International Journal of Chemical Engineering*, vol. 2012, 2012, doi: 10.1155/2012/569463.
- [65] X. Tao, Y. Liu, H. Jiang, and R. Chen, "Microbubble generation with shear flow on large-area membrane for fine particle flotation," *Chemical Engineering and Processing - Process Intensification*, vol. 145, no. June, p. 107671, 2019, doi: 10.1016/j.cep.2019.107671.
- [66] Q. Xu, M. Nakajima, S. Ichikawa, N. Nakamura, and T. Shiina, "A comparative study of microbubble generation by mechanical agitation and sonication," *Innovative Food Science and Emerging Technologies*, vol. 9, no. 4, pp. 489–494, 2008, doi: 10.1016/j.ifset.2008.03.003.
- [67] Y. Lecoffre and J. Marcoz, "Micro-bubble Injector," US4556523, 1985.
- [68] R.-H. Yoon, G. T. Adel, and G. H. Luttrell, "Process and apparatus for separating fine particles by microbubble flotation together with a process and apparatus for generation of microbubbles," US4981582A, 1991.
- [69] P. Gordiychuk, A., Svanera, M., Benini, S., Poesio, "Size Distribution and Sauter Mean Diameter of Microbubble for a Venturi Type Bubble Generator," *Experimental Thermal and Fluid Science*, vol. 70, no. January, pp. 51–60, 2016, doi: 10.1016/j.expthermflusci.2015.08.014.
- [70] G. Khirani, S., Kunwapanitchakul, P., Augir, F., Guigui, C., Guiraud, P., Hebrard, "Microbubble generation Through Porous membrane Under Aqueous or Organic Liquid Shear Flow," *Industrial & Engineering Chemistry Research*, vol. 51, no. 4, pp. 1997–2009, 2012, doi: 10.1021/ie200604g.
- [71] N. Suwartha, D. Syamzida, C. R. Priadi, S. S. Moersidik, and F. Ali, "Effect of size variation on microbubble mass transfer coefficient in flotation and aeration processes," *Heliyon*, vol. 6, no. 4, p. e03748, 2020, doi: 10.1016/j.heliyon.2020.e03748.
- [72] B. Swart *et al.*, "In situ characterisation of size distribution and rise velocity of microbubbles by high-speed photography," *Chemical Engineering Science*, vol. 225, p. 115836, 2020, doi: 10.1016/j.ces.2020.115836.
- [73] Y. Bao, S. Tong, J. Zhang, Z. Cai, and Z. Gao, "Reactive mass transfer of single bubbles in a turbulent flow chamber: Discussion on the effects of slippage and turbulence," *Chemical Engineering Science*, vol. 231, p. 116253, 2021, doi: 10.1016/j.ces.2020.116253.

- [74] S. Balamurugan, M. D. Lad, V. G. Gaikar, and A. W. Patwardhan, "Hydrodynamics and mass transfer characteristics of gas-liquid ejectors," *Chemical Engineering Journal*, vol. 131, no. 1–3, pp. 83–103, 2007, doi: 10.1016/j.cej.2006.12.026.
- [75] K. Amagai and K. Tabei, "Atomization Characteristics of Liquid Containing Micro-Bubbles," in *ICLASS-2006*, 2006, pp. 1–5.
- [76] S. Haris, X. Qiu, H. Klammler, and M. M. A. Mohamed, "The use of micro-nano bubbles in groundwater remediation: A comprehensive review," *Groundwater for Sustainable Development*, vol. 11, no. October, p. 100463, 2020, doi: 10.1016/j.gsd.2020.100463.
- [77] A. Paramesti et al., "Development of Low-Cost Aerobic Bioreactor for Decentralized Greywater Treatment," *Advances in Waste Processing Technology*, pp. 111–125, 2020, doi: 10.1007/978-981-15-4821-5\_7.
- [78] Y. M. Lau, N. G. Deen, and J. A. M. Kuipers, "Development of an image measurement technique for size distribution in dense bubbly flows," *Chemical Engineering Science*, vol. 94, pp. 20–29, 2013, doi: 10.1016/j.ces.2013.02.043.
- [79] S. Liu, L. le Yang, D. Zhang, and J. yu Xu, "Separation characteristics of the gas and liquid phases in a vane-type swirling flow field," *International Journal of Multiphase Flow*, vol. 107, pp. 131–145, 2018, doi: 10.1016/j.ijmultiphaseflow.2018.05.025.
- [80] J. C. Lasheras, C. Martínez-Bazán, and J. L. Montañés, "On the breakup of an air bubble injected into a fully developed turbulent flow. Part I: Breakup frequency," *30th Fluid Dynamics Conference*, no. 1949, 1999, doi: 10.2514/6.1999-3642.
- [81] T. S. Kress and J. J. Keyes, "Liquid phase controlled mass transfer to bubbles in cocurrent turbulent pipeline flow," *Chemical Engineering Science*, vol. 28, no. 10, pp. 1809–1823, 1973, doi: 10.1016/0009-2509(73)85063-8.
- [82] R. T. Rodrigues and J. Rubio, "New basis for measuring the size distribution of bubbles," *Minerals Engineering*, vol. 16, no. 8, pp. 757–765, 2003, doi: 10.1016/S0892-6875(03)00181-X.
- [83] H. S. Tapia, J. A. G. Aragón, D. M. Hernández, and B. B. García, "Particle Tracking Velocimetry (PTV) Algorithm for Non-uniform and Nonspherical Particles," *Proceedings of the Electronics, Robotics and Automotive Mechanics Conference (CERMA'06)*, 2006.
- [84] C. Nagabathula, "Multiphase Flow Metering Using a Pressure Drop Based Metering Device," no. April, 2018, [Online]. Available: <https://dalspace.library.dal.ca/xmlui/handle/10222/73897?show=full>.
- [85] J. Cheng et al., "A novel jet-aerated tangential swirling-flow plate photobioreactor generates microbubbles that enhance mass transfer and improve microalgal growth," *Bioresource Technology*, vol. 288, no. April, p. 121531, 2019, doi: 10.1016/j.biortech.2019.121531.
- [86] X. Wang et al., "Bubble breakup in a swirl-venturi microbubble generator," *Chemical Engineering Journal*, vol. 401, no. January, 2021, doi: 10.1016/j.cej.2020.126397.
- [87] L. Liu and B. Bai, "Numerical study on swirling flow and separation performance of swirl vane separator," *Interfacial Phenomena and Heat Transfer*, vol. 5, no. 1, pp. 9–21, 2017, doi: 10.1615/InterfacPhenomHeatTransfer.2018021108.
- [88] L. Sun et al., "Characteristics and mechanism of bubble breakup in a bubble generator developed for a small TMSR," *Annals of Nuclear Energy*, vol. 109, pp. 69–81, 2017, doi: 10.1016/j.anucene.2017.05.015.
- [89] H. S. Alam, G. G. Redhyka, Bahrudin, A. T. Sugiarto, T. I. Salim, and I. R. Mardhiya, "Design and Performance of Swirl Flow Microbubble Generator," *International Journal of Engineering & Technology*, vol. 7, no. 4.40, pp. 66–69, 2018, doi: 10.14419/ijet.v7i4.40.24077.
- [90] A. Basso, F. A. Hamad, and P. Ganesan, "Effects of the geometrical configuration of air–water mixer on the size and distribution of microbubbles in aeration systems," *Asia-Pacific Journal of Chemical Engineering*, vol. 13, no. 6, pp. 1–11, 2018, doi: 10.1002/apj.2259.
- [91] S. Huang, X. Su, J. Guo, and L. Yue, "Unsteady numerical simulation for gas-liquid two-phase flow in self-priming process of centrifugal pump," *Energy Conversion and Management*, vol. 85, pp. 694–700, 2014, doi: 10.1016/j.enconman.2014.03.023.
- [92] H. Kudela and A. Kosior, "Numerical study of the vortex tube reconnection using vortex particle method on many graphics cards," *Journal of Physics: Conference Series*, vol. 530, no. 1, 2014, doi: 10.1088/1742-6596/530/1/012021.

- [93] J. T. Kuo and G. B. Wallis, "Flow of bubbles through nozzles," *International Journal of Multiphase Flow*, vol. 14, no. 5, pp. 547–564, 1988, doi: 10.1016/0301-9322(88)90057-2.
- [94] P. M. Wilkinson, A. Van Schayk, J. P. M. Spronken, and L. Van Dierendonck, "The influence of gas density and liquid properties on bubble breakup," *Chemical Engineering Science*, vol. 48, no. 7, pp. 1213–1226, 1993, doi: 10.1016/0009-2509(93)81003-E.